ISSN (Online) 2395-2717

International Journal of Engineering Research in Electrical and Electronic Engineering (IJEREEE)
Vol 3, Issue 12, December 2017

A Modified P&O Maximum Power Point Tracking Method with Reduced Steady State Oscillation and Improved Tracking Efficiency

[1] V.Poojitha, [2] J.Suresh

***Abstract:*-- This work proposes a method to reduce the steady state oscillation and to mitigate the probability of losing the tracking direction of the perturb and observed (P&O) based maximum power point tracking (MPPT) for PV system. The modified scheme retains the conventional P&O structure, but with a unique technique to dynamically alter the perturbation size. At the same time, a dynamic boundary condition is introduced to ensure that the algorithm will not diverge from its tracking locus. The modified P&O is simulated in Matlab Simulink and its performance is benchmarked using the standard MPPT efficiency (ηMPPT) calculation. Furthermore, the proposed concept is validated experimentally using a buck-boost converter, fed by a solar PV array simulator (PVAS). Based on the EN 50530 dynamic irradiance tests, the proposed method achieved an average ηMPPT almost 1.1% higher than the conventional P&O when irradiance changes slowly and about 12% higher under fast change of irradiance.**

Keywords: MPPT, PV, Solar, P&O, tracking MPP, P-V curve

I. INTRODUCTION

For a long term and sustainable supply of energy, it is essential to exploit and utilize the renewable sources at a much larger scale. Among the renewables, the solar photovoltaic (PV) is expected to be among the most prominent due to its abundance, ease of installation and almost maintenance free. In addition, it is considered as green energy and thus addresses the concerns over the environment. However, due to the low conversion efficiency of the PV modules, the cost of solar power is still higher relative to the fossil fuel. One effective way to increase the efficiency is to improve its maximum power point tracking (MPPT) algorithm. Since the MPPT comprises of software codes, this approach appears to be the most economical way to enhance the energy throughput.

The function of MPPT is to ensure that the operating voltage and current always stay at the maximum power point (MPP) on the P-V characteristic curve. To date, numerous MPPT techniques are reported in literature [1-3]; they are broadly classified into two categories, namely the conventional and soft computing approach. The most popular conventional MPPT are the perturb and observe (P&O) [4, 5], hill climbing [6] and incremental conductance [7]. These algorithms are widely used in commercial products—mainly due to their simplicity and robustness. On the other hand, soft computing based MPPT such as artificial neural network [8], fuzzy logic [9], differential evolution [10], particle swarm optimization [11, 12] and cuckoo search [13] tend to be more versatile and flexible. Despite exhibiting better steady state performance, they are much slower and in practice, are not as acceptable.

Among the conventional MPPT, P&O is the simplest and exhibits very good convergence. However, the algorithm suffers from two serious drawbacks. First is the continuous oscillation that occurs around the MPP. Second, the P&O is prone to lose its tracking direction when the irradiance (G) increases rapidly. Both problems contributes to the loss of power and hence reduced tracking efficiency. Although there exists several work that address the oscillation issue using the adaptive P&O schemes [14-18], none has comprehensively address the loss of tracking direction–despite it being highlighted by [1, 5]. Notwithstanding this, authors in [19-21], have introduced several solutions to address these two problems. However, the methods are limited for specific conditions as shall be discussed in Section II. With this hindsight, this work proposes a more comprehensive modification to the P&O, with the aim to solve both problems simultaneously. The modified algorithm maintains a similar structure to the conventional P&O, but it incorporates a unique dynamic perturbation to decrease the oscillation, while maintaining a reasonable convergence time. In addition, the method introduces boundary conditions on the P-V curve that prevents the operating point from being diverged (uncontrollably) from the MPP.

Another issue that has been neglected is the performance benchmarking of the MPPT algorithms. In almost all publications, the P&O are tested against very simple irradiance profiles—which in most cases do not reflect the

ISSN (Online) 2395-2717

International Journal of Engineering Research in Electrical and Electronic Engineering (IJEREEE)
Vol 3, Issue 12, December 2017

conditions that occur in the real environment. Consequently, the margin of improvement between the conventional and adaptive P&O is not very significant. In this work, the conventional as well as the modified P&O is comprehensively benchmarked using the EN 50530 dynamic MPPT efficiency test. This test is very rigorous as it demands the algorithm to track a set of irradiance ramps with variable rate of change [22]. The results for the conventional and modified P&O is compared side by side and the performance enhancement due to the proposed method is clarified.

PRIOR ART IN ADAPTIVE P&O

[4] Limitations of the Conventional P&O

In the conventional P&O, the power (P) is computed using the sensed values of the voltage and current of the PV array. Then a perturbation (ΔX), which is based on the change in P is provided, i.e.

$$X_{new} = X_{old} + \Delta X \times \phi \quad (1)$$

In (1), X is the controlled variable of the MPPT, while X is the perturbation step size. The controlled variable can be either duty cycle (d), voltage (V) or current (I); correspondingly, the perturbation is d, V or I, respectively. The multiplier ϕ indicates the direction of perturbation: +1 and –1 for an increasing and decreasing value of X, respectively. If the perturbation results in an increase in power, the polarity of ϕ is maintained until it reaches MPP. Once that point is crossed, the power decreases. Thus, ϕ is reversed and the algorithm climbs towards the MPP from the opposite direction of the P-V curve. Due to this action, the operating point moves back and forth around the MPP, causing an oscillation in the output power. The size of X, is crucial; if X is large, the convergence is fast—but it results in large oscillation and vice versa.

Apart from the oscillation at steady state, it is also possible for the P&O to lose its tracking direction, i.e. diverging away from the MPP. This normally happens when a fast and continuous increase of G (or the gradient of the ramp of G) takes place [1]. The phenomena can be explained with the aid of Fig. 1. Assume initially, the algorithm locates the MPP at point A. Expectedly, the operating point oscillates between A, B and B'. Now, consider the case while moving from B' to A, G increases quickly. In this situation, it is possible for the operating point to move towards C, instead of B. This happens if the algorithm sees that the present perturbation results in the increase in power. Because of that, it keeps on providing a perturbation in the same direction. The operating point follows the path A-C-D-E, which is towards the left of the P-V curve, as shown in Fig. 1(a). As can be seen, due to this action, the operating point diverges away from the MPP. The second possibility is that G changes while the perturbation causes the operating point to move from B to A. In this case, the next perturbation is in the same direction, i.e. in the direction of increasing power. Clearly, the operating point moves towards the right side of the P-V curve—following the path A-C'-D'-E', as shown in Fig. 1(b).

Clearly the divergence results in the loss of MPP tracking and hence a drop in the MPPT efficiency [1, 5]. The problem is particularly acute when G changes with high gradient (10 to 100 W/m^2/s). However, it must be noted that, the possible loss of tracking direction only occurs when G is ascending. When descending, the same phenomenon does not take place [23].

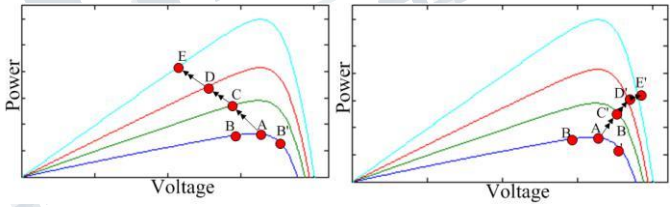

(a) (b)

Fig. 1. The losing of the tracking direction by conventional P&O (a) towards the left (b) towards the right of the P-V curve.

B. Mitigation Methods Using Adaptive P&O

The two limitations of the conventional P&O, namely the oscillation and loss of tracking direction are addressed using the adaptive P&O approach [14, 17-20, 24, 25]. The voltage is the most common variable used for adaptation. In this case, the voltage perturbation size (V) is reduced as the operating voltage gets closer to MPP. The manner in which the perturbation is reduced differentiates the performance of one scheme to another. For example, in [24], V is initially set to 10% of the open circuit voltage (V_{oc}). It is gradually reduced to 0.5% of V_{oc} once it reaches the vicinity of MPP. In another approach [25], the perturbation size is being made adaptive using,

$$\Delta V = M \Delta P$$

ISSN (Online) 2395-2717

International Journal of Engineering Research in Electrical and Electronic Engineering (IJEREEE)
Vol 3, Issue 12, December 2017

$$\Delta V_{n+1} = \frac{\Delta P_n}{\Delta V_n} \quad (2)$$

where, P is the change in power and M is a user-depended constant that requires tuning. When the level of G increases drastically, P becomes large but V remains small. Consequently, the ratio of P to V (which is the perturbation size) becomes very large momentarily, resulting in the loss of tracking for a certain duration. To avoid such occurrence, a logarithmic function is used in [14], i.e.

$$\Delta V_{n+1} = M \log_{10}\left(\left|\frac{\Delta P_n}{\Delta V_n}\right|\right) \quad (3)$$

The logarithm keeps the perturbation size small even if the ratio of P to V gets large. Note that, despite the ability of the schemes in [14, 24, 25] to reduce the oscillation, they still suffer from the tracking deviation when G increases quickly.

In [19], the authors managed to effectively track the gradient of G using the PI voltage controller, followed by a (inner-loop) current controller. Furthermore, the perturbation (V) is reduced to zero when the steady state oscillation is detected. As the oscillation is completely removed, the MPPT no longer provides any perturbation until a considerable change in I_{pv} takes place. However this is not always the case. For example, a slow change in T and G results in a slow change in I_{pv}, which in turn causes the I_{pv} to remain below the threshold. Since V is already gone to zero, the MPPT algorithm will force the operating point to remain at the same voltage despite the fact that the actual V_{MPP} has changed its position. Consequently, there will be an MPP mismatch,
which results in power loss.
In [20, 26], the authors utilize the fact that the current perturbation (ΔI) is proportional to the change of G. The MPPT response is very fast, particularly when G jumps from one level to another. However, the method requires an expensive measurement of G using sensors. Furthermore, the authors did not address the divergence issue.
In [17, 18, 27-29], the duty cycle (d) based adaptive P&O schemes are proposed. Again, it has to be noted, however, these methods are related to the reduction of the steady-state oscillation; they do not prevent the algorithm from diverging away from the MPP. However, in [21], the authors attempt to capitalize the adaptive P&O to simultaneously resolve the divergence issue by deducing that when G is increasing and if
V > 0 and I > 0, then ϕ should be +1. However, this observation is only true when the algorithm attempts to diverge to the right. However, if it attempts to diverge to the left i.e. V < 0 and I > 0, the method does not work. This is because, the MPPT keeps providing perturbation to the left and consequently MPPT diverges in that direction. Besides that, only a single ramp, i.e. with a gradient of 210 W/m2/s is used to validate the result.
From this brief overview, it can be concluded that there is a literary gap concerning the divergence problem of the P&O. The prior schemes that attempt to resolve this issue exhibit limitations under specific conditions, as described above. Besides, none of them has proven their effectiveness using multiple gradients G tests, such as the EN 50530 Standard profiles.

III. PV MODELING

The main purpose of modeling is to emulate the behavior of the PV modules, so that it can be integrated with the electrical-based software, such as MATLAB/Simulink. In this work, the two diode model [30] is used. This model is fast and offers improved result, especially under low G. To maintain simplicity, the popular series-parallel interconnection is utilized. For a PV system which comprises of NS and NP modules connected in series-parallel, the equivalent circuit (utilizing the two diode model) is shown in Fig. 2.

Fig. 2. The two-diode model with the series-parallel combination
If V is the PV voltage, and N=NS/NP then the current drawn from the system can be written as
where Rs and Rp are the series and parallel resistance, respectively, while VT is the thermal voltage of the diodes and a1 and a2 are the ideality factor for the diode 1 and 2 respectively. The light generated current (IPV) is given by
Where, G and T represent irradiance and temperature respectively. Note that IPV_STC and other variables with the same subscript are measured in the standard test condition (STC) 1 . Variable KI is the short circuit current coefficient, which is usually provided by the manufacturer. The diode saturation current is given by

ISSN (Online) 2395-2717

International Journal of Engineering Research in Electrical and Electronic Engineering (IJEREEE)
Vol 3, Issue 12, December 2017

In Eq. (8), Isc and Voc are the short circuit current and the open circuit voltage in STC, respectively. Variable KV is the temperature coefficient of the voltage. The specifications for the PV module (MSX 60) [31] used in this paper are given in

TABLE I.
TABLE I: The specifications of the PV module (MSX 60)

Parameters	Label	Value
Short Circuit current	I_{SC}	3.8 A
Open circuit voltage	V_{OC}	21.1 V
Current at Pmax	I_{MPP}	3.5 A
Voltage at Pmax	V_{MPP}	17.1 V
Maximum power	P_{MPP}	59.85 W
V_{OC} coef. of temperature	K_V	-0.08 V /^{0}C
I_{SC} coef. of temperature	K_I	$3e^{-3}$ A / ^{0}C
cell in series per module	n	36

IV. THE PROPOSED MODIFIED P&O

A. Concept

The objective of the modified P&O is to ensure that steady state oscillation and the deviation from the tracking locus is minimized. As usual, it begins by tracking uniform G. After going through a few perturbation cycles, the operating point should reach near the MPP. By then the oscillation around the MPP takes effect. It is detected by an intelligent check (which shall be described later), where the perturbation size is reduced to a minimum value. Using this procedure, the problem of oscillation is resolved.

The loss of tracking direction is addressed as follows. While the tracking continues, the amount of normalized power change (ΔP/P) is measured and compared with a threshold value, Tr. If P/P < Tr, then it can be concluded that the change in power is not sufficiently big, an indication that G is changing slowly. In this case, the perturbation size is kept minimum as it is sufficient to handle the slow change of G. Otherwise, if P/P > Tr perturbation is increased to ensure that operating point can cope with the gradient of G. To avoid be forced to remain always inside the boundary and not get diverged from the MPP region. However when the change of *G* finally stops, the algorithm will settle at the MPP. Afterwards around the MPP, it will detect the oscillation and reduce the perturbation size to the minimum level.

B. Adaptive Perturbation Size

Based on the observation by numerous research [32, 33] that the MPP lies in the vicinity of $0.8\times V_{oc\_array}$ ($V_{oc\_array}=V_{oc}\times N_S$). Thus the initial searching point for the MPPT is set to $0.65\times V_{oc\_array}$. The reason for setting the initial value to be slightly away from the MPP is to record the gradient (ϕ) (positive or negative) of the *P-V* curve, i.e. *P* and *V*. The "*value*" of ϕ is the sign multiplication of these two quantities and normalized to unity, as shown in TABLE II. These values will be later used to determine if the algorithm has converged to MPP and hence variation of the perturbation size.

TABLE II: Determination of the ϕ values

P	*V*	ϕ value
+	+	+1
+	–	–1
–	+	–1
–	–	+1

The oscillation is detected by recording the five consecutive values of the ϕ. During the increase or decrease of the voltage, the five consecutive ϕ are either positive or negative, respectively. Thus, the absolute value of the summation of all five ϕ is 5. After reaching the MPP, the oscillation starts; the operating point will move two times in one direction and then move to the opposite direction. As a result, the absolute value of the summation of the five ϕ is always less than 5. Accordingly, by recording five consecutive ϕ it is possible to detect the occurrence of oscillation precisely, i.e.

$$if \sum slope = \begin{cases} 5 \text{..... [MPPT not converged to steady state]} \\ < 5 \text{..... [MPPT converged to steady state]} \end{cases} \quad (9)$$

The initial perturbation size is set to $0.02\times V_{oc\_array}$ (2% of V_{oc_array}). According to [34], this value is well optimized. Meanwhile, when the oscillation is detected, the size of the perturbation is reduced by 0.5% of V_{oc_array} in every iteration. The perturbation size is continuously reduced until it reaches 0.5% of V_{oc_array} at steady state. Although the algorithm could not converge to a single MPP point, the perturbation size is small enough thus oscillation is very small, resulting in almost negligible power loss.

There is an important reason for not allowing the perturbation to be zero. In reality, there is always small fluctuations in *G*. Besides, the change of *T* occurs very slowly and it is acknowledged that the position of the MPP varies with *T* significantly [2]. Since a small change in *G* and a slow change of *T* do not induce a sudden change in the power, assigning the zero perturbation will force the MPPT to track the same voltage all over the

ISSN (Online) 2395-2717

International Journal of Engineering Research in Electrical and Electronic Engineering (IJEREEE)
Vol 3, Issue 12, December 2017

period. It can cause severe efficiency drops, because while the MPPT sticks to the same operating point, the exact MPP position keeps moving away. Thus, it is crucial to maintain the perturbation at a small value, rather than zero. However it must be small enough to keep the oscillation to a very low value, such that the power loss is negligible.

C. Eliminating the Possible Loss of Tracking Locus

In the real environment, G varies in two possible ways, i.e. slow (approximately 1 ~ 10 W/m^2/s) or fast (≥ 10 W/m^2/s). For the conventional P&O, both are treated equally due of its fixed perturbation step size. If the change is slow, the gradient of G is not steep. Thus, it is very likely for the conventional algorithm to cope with the changes. However, for fast rising gradient, the probability of losing track increases, as explained in Section II.

Fig. 3 depicts the mechanism in which the modified P&O eliminates the possible loss of tracking direction. First a flag called *steady_flag* is introduced. Initially, *steady_flag*=0; but once the algorithm detects the steady state oscillation, it is toggled to 1. Next, a boundary condition for the voltage is imposed. At the beginning, a voltage range is set to [0.5V_{oc} to 0.95V_{oc_array}]. When the *steady_flag*=1 is detected (which means that the oscillation has occurred), the boundaries are changed to [V^*_{mpp}–0.05×V_{oc_array} to V^*_{mpp}+0.05×V_{oc_array}]. Note that V^*_{mpp} is the target MPP voltage. These boundaries are selected because when G increases, the V^*_{mpp} actually shifts slightly to the right. The shifting is observed to be approximately 5% of V_{oc_array}, as depicted by Fig. 3. Thus by restricting V^*_{mpp} within the 5% margin, the operating point is forced to remain near the MPP—thus avoiding the loss of tracking locus.

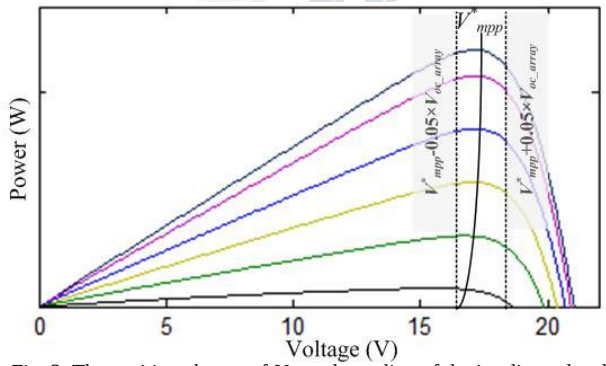

Fig. 3. The position change of V_{MPP} depending of the irradiance level

Within the imposed boundary, the algorithm tracks the MPP using either the minimum perturbation or the maximum perturbation. The latter equals to the initial perturbation. If the gradient of G is low, the minimum perturbation is maintained. On the other hand, if the gradient is high, the perturbation size is restored to the initial size. Despite the need to know the irradiance value, the method does not require a direct measurement for the change of G using irradiance sensors. Instead, the following procedure is used. When G starts changing and the MPPT takes two consecutive samples, it is assumed that T will remain almost at the same values. From (7), if T remains constant in two consecutive samples, the two samples for the PV current, I_{pv1} and I_{pv2} respectively can be written as follows:

$$I_{pv1} = \left(I_{pv\_STC} + K_I\left(T - T_{STC}\right)\right)\frac{G_1}{G_{STC}} \quad (10)$$

$$I_{pv2} = \left(I_{pv\_STC} + K_I\left(T - T_{STC}\right)\right)\frac{G_2}{G_{STC}} \quad (11)$$

Dividing (11) by (10) results in the following relationship

$$\frac{I_{pv2}}{I_{pv1}} = \frac{G_2}{G_1} \quad (12)$$

For the two consecutive voltage samples V_1 and V_2, it can be assumed that $V_2 = V_1 \pm \Delta V$. Since $V \ll V_1$, thus $V_2 \approx V_1$. Consequently (12) can be approximated as below

$$\frac{V_2 I_{pv2}}{V_1 I_{pv1}} \approx \frac{G_2}{G_1} \quad (13)$$

or

$$\frac{P_2}{P_1} = \frac{G_2}{G_1} \quad (14)$$

Alternatively (14) can be expressed as

$$\frac{P_2 - P_1}{P_1} = \frac{G_2 - G_1}{G_1} \quad (15)$$

Recognizing that P_2-P_1 is the change in power P, (15) can be written as

$$\frac{\Delta P}{P_1} = \frac{\Delta G}{G_1} \quad (16)$$

From (16), it can be deduced that the normalized change in power is equivalent to the normalized change in G. Since the continuous power is being measured, this information can be used to determine the change in G. For example, in a change of G with the gradient 10 W/m^2/s; thus G= 10W/m^2. At STC

ISSN (Online) 2395-2717

International Journal of Engineering Research in Electrical and Electronic Engineering (IJEREEE)
Vol 3, Issue 12, December 2017

(G_1=1000W/m^2), P/P (which is equivalent to G/G) is expected to be 0.01 in every two samples.

As presented in [34], the divergence problem of the P&O is prominent when the gradient, i.e. $G/\Delta t \geq 10$ W/m^2/s. Below this value, the irradiance increase in every second is slow (less than 10 W/m^2) so as change the position of the actual MPP.

Such slow varying MPP can be tracked using the minimum perturbation size. However, if $G/\Delta t \geq 10$ W/m^2/s, the perturbation size must be increased in order to track the MPP, hence the justification for G/G= 0.01. Accordingly, this value is selected as the threshold T_r. If the normalized power change is equal or greater than 0.01, the perturbation size is

A. Algorithm Flowchart

The complete flowchart of the modified P&O scheme is presented in Fig. 4. First, the initializing and assigning of variables are carried out. The open circuit voltage of each resumed to the initial value; otherwise it is kept to the minimum value.

Thus the probability of losing the track of the MPP is avoided. Meanwhile, the present value of the V*mpp is sent to the output as Vout.

V. IMPLEMENTATION

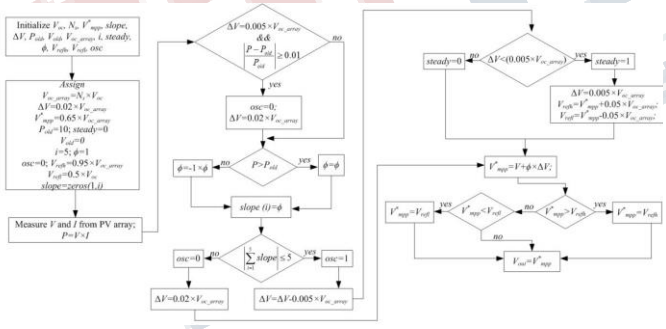

Fig.4. The complete flowchart of the Modified P&O

. Experimental Set-up

Fig. 5(a) presents the Matlab simulation platform to realize the modified P&O algorithms. The PV array simulator adopts the two diode model configuration. The value of T and G is fed into the simulator and the PV current is delivered to the converter. The buck-boost dc to dc converter is used to convert the output voltage of the MPPT to the load voltage. The converter is designed to

perturbation occurs in the same direction. Thus it can be concluded that the oscillation around the MPP has not taken place. Consequently, the algorithm considers V_{mpp} as the output of the MPPT algorithm. In this case, the perturbation size remains at 2% of V_{oc_array}. On the contrary, if the values inside the gradient array are not equal, it is an indication that the operating point is oscillating around the MPP. Accordingly the divergence from th

following specifications: switching frequency (f) = 50 kHz, inductor (L) = 1 mH and capacitor C_1 = 470 µF and C_2 = 220 µF. At the input side, the PV voltage and the current are measured using the voltage and the current sensor, respectively. Using these measured values, the respective MPPT algorithm generates V_{out}. Then the V_{ref} subtracted from the V_{out}; the difference is the error voltage V_{error}, which is then fed to a proportional-integral (PI) controller. The output of the PI controller is compared to a saw tooth waveform to produce the required duty cycle (D) for the converter. This duty cycle forces the converter to operate at the desired PV voltage, i.e. at the V_{MPP}.

The similar configuration is maintained in the hardware presented in Fig. 5(b). In the hardware instead of using real PV arrays a custom designed PV Array Simulator (PVAS) [35] is used. The simulator consists of a linear, high-voltage MOSFET-based power stage and a special current controller. It provides real-time generation capabilities of any time series of G, T and fill factor. The P&O and modified algorithm is implemented by the TMS320F240 DSP on the Dspace DS1104 platform [36]. The voltage and current from the converter side are measured by the voltage and the current sensors and recorded by PVAS data logger and oscilloscope. minimum value.

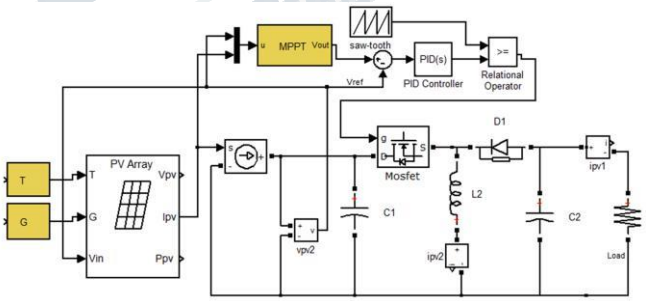

(a)

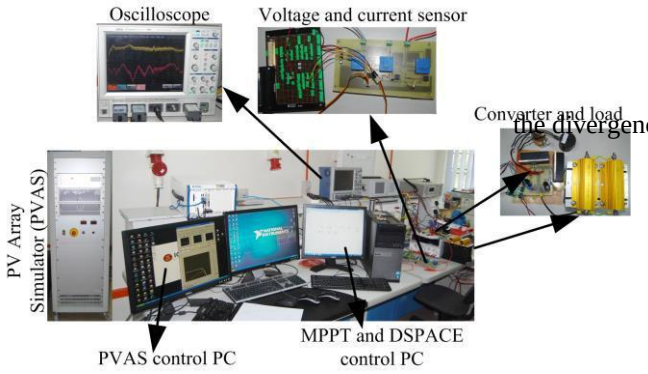

ISSN (Online) 2395-2717

International Journal of Engineering Research in Electrical and Electronic Engineering (IJEREEE)
Vol 3, Issue 12, December 2017

(b)

Fig. 5. (a) The Matlab simulation platform (b) The Hardware setup

VI. Results and Discussions

A. Performance Evaluation

The effectiveness of the MPPT algorithm is benchmarked using the MPPT efficiency formula, i.e.

$$\eta_{MPPT} = \frac{P_{out}(t)}{P_{\max}(t)} \quad (17)$$

and the average efficiency is calculated using

$$\eta_{MPPT,avg} = \frac{\int P_{out}(t)dt}{\int P_{\max}(t)dt} \quad (18)$$

In (17) and (18), P_{max} is the possible (theoretical) achievable power, computed using the Eqs. (4)–(8). On the other hand,

P_{out} is the power extracted from the PV array by the algorithm—which depends upon the ability of the MPPT to be

as close as possible to the MPP. To calculate the P_{out}, the array voltage and the current are measured using sensors and then multiplied. Note that the η_{MPPT} is not concerned about the physical efficiency of the converter (for example switching loss, turn-on loss etc.).

B. The EN 50530 MPPT Efficiency Test

The EN 50530 [20] is a standard test to determine the dynamic MPPT efficiency. It is carried out using series of irradiance triangular waveforms with different values of gradients (ramps): from 0.5 W/m^2/s to 100W/m^2/s. Thus, the profile covers a comprehensive range of irradiance change, i.e. from very slow (almost at steady state) to very fast (almost a step change), as illustrated in the Fig. 6(a). In this work, the EN50530 is used in a slightly modified form: 1) the startup and closing ramps are ignored; these ramps are required for the inverter but not a prerequisite for the MPPT efficiency computing, 2) the same ramp signal is not repeated (as in the original EN50530 document) because it is known that the MPPT algorithm responds identically for the same ramp. Despite these omissions, the validity of the computed MPPT efficiency is not affected in any way. The resulting tracking performance of the conventional and the modified P&O is presented in Fig. 6(b). Certain parts of the waveform are enlarged for clarity. During the very slow change of G (at the beginning of the profile, 0.5 W/m^2/s), the tracking by the modified P&O is almost perfect—as illustrated by the enlarged image 1.

This can be attributed to the fact that the slow ramp almost resembles a steady state condition, in which the variable perturbation sizing is activated. On the other hand, the conventional P&O exhibits considerable oscillation due to the large and fixed perturbation size. However, there is no visible loss of tracking direction because it is still able to cope with the (slow) change of G. As the ramp gradient becomes steeper, the tendency of losing the tracking direction increases, as depicted in the image 2. As can be observed, the conventional P&O diverged from the tracking locus a number of times when the ramp is at 14 W/m^2/s. When the steepness increases further, the divergence worsens.

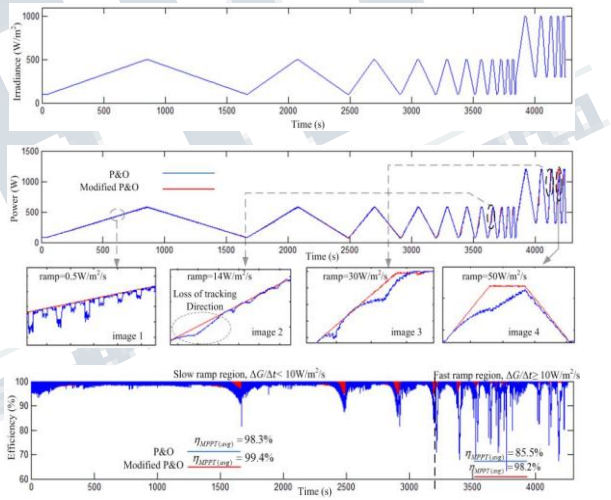

Fig. 6. (a) The irradiance profile for the EN50530 test (b) The tracking performance of the conventional P&O and the modified P&O (c) Efficiency of the conventional P&O and the modified P&O

This condition can be verified by observing images 3 (20 W/m2/s) and 4 (50 W/m2/s), respectively. For the latter, the peak of the ramp is unreachable, which can be considered as losing the tracking completely. On the contrary, the modified P&O tracks all the ramps with high precision over the entire profile.

The effects of the oscillation and losing the tracking capability are manifested in the efficiency graph, i.e. Fig 6(c). In the slow ramp region (with the rate of change in G/Δt< 10 W/m2/s), the ηMPPT(avg) for the conventional

ISSN (Online) 2395-2717

International Journal of Engineering Research in Electrical and Electronic Engineering (IJEREEE)
Vol 3, Issue 12, December 2017

P&O and the modified P&O is 98.3% and 99.4%, respectively. This difference is mostly due to the steady state oscillation. However, when G changes quickly (i.e. the ramp gradient is higher than 10 W/m2/s), the conventional P&O lose its tracking much more frequently. As a result, in this region, the efficiency drops considerably. In certain parts of the profile, the efficiency is extremely volatile—recording values of ηMPPT < 70%. In average, the computed ηMPPT(avg) of the conventional P&O for this region is 85.5%. On the other hand, for the modified P&O, the tracking performance is very consistent. Its ηMPPT ranges between 97.5% to 99.4%, while its ηMPPT(avg) is computed to be 98.2%, This efficiency is approximately 12% higher than the conventional P&O. On the overall, the average ηMPPT for the total profile (which includes the slow and the fast ramp regions) is 96.2% and 99.1% for the conventional P&O and the modified P&O respectively—an improvement of nearly 3%.

C. Experimental Verification

To prove correctness of the proposed MPPT algorithm, an experimental verification is carried out. The waveforms of two selected ramps are shown in Figs. 7 through 10. In Figs. 7(a) and (b), the simulated and practical performance of the conventional P&O for the 30 W/m2/s ramp is illustrated. In these figures, the dotted line represents the actual VMPP and PMPP that the voltage and power locus should follow. It can be observed that, in the voltage (in both simulation and hardware) is diverging away from the dotted line continually. Note that the divergence can occur on the left or the right side of the MPP, as depicted by Fig. 1. In the simulation, i.e. Fig 7(a), the divergence is on the left side of the MPP. This can be confirmed by the large dip in the voltage. During this interval, the power diverges significantly form the intended locus (dotted line). For the experiment, the divergence is on the right side of the MPP. This can be determined by observing the oscillogram, which indicates a voltage rise Furthermore, it should be understood that the direction of the divergence is a phenomenon that cannot be controlled. It depends on the direction of the perturbation at the moment when G starts ascending.

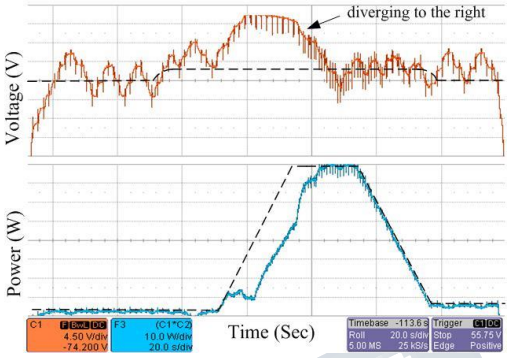

Fig. 7. The tracking performance of the conventional P&O for the 30 W/m2 ramp; (a) simulation (b) experimental

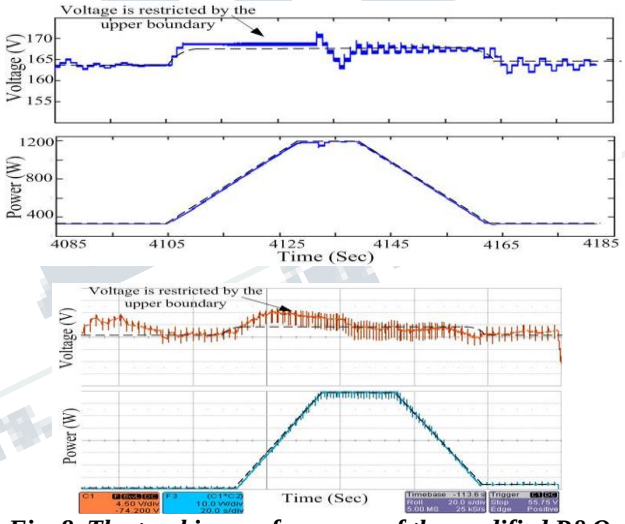

Fig. 8. The tracking performance of the modified P&O for the 30 W/m2 ramp; (a) simulation (b) experimental

However, it can be seen that the period at which the divergence occurs is consistent for both simulation and hardware, thus proving its correctness. In addition, regardless of the direction of the diverging voltage, the locus of the power divergence remains similar. It is due to this large power divergence, the MPPT efficiency drops to nearly 75%, as indicated in Fig. 6 (c).

Fig. 8 shows the tracking performance when the modified P&O is applied. As expected, it tracks the power locus almost perfectly, as shown in Fig. 8 (a) and (b), for simulation and experimental, respectively. The underlying reason for this excellent tracking can be traced from the

ISSN (Online) 2395-2717

International Journal of Engineering Research in Electrical and Electronic Engineering (IJEREEE)
Vol 3, Issue 12, December 2017

voltage profile. During the ascending change of G, the voltage is restricted within the upper boundary imposed by the algorithm. Thus the operating point is forced to stick near the MPP. As a result, there is a negligible deviation in the power. However it has to However, it can be seen that the period at which the divergence occurs is consistent for both simulation and hardware, thus proving its correctness. In addition, regardless of the direction of the diverging voltage, the locus of the power divergence remains similar. It is due to this large power divergence, the MPPT efficiency drops to nearly 75%, as indicated in Fig. 6 (c).

Fig. 8 shows the tracking performance when the modified P&O is applied. As expected, it tracks the power locus almost perfectly, as shown in Fig. 8 (a) and (b), for simulation and experimental, respectively. The underlying reason for this excellent tracking can be traced from the voltage profile. During the ascending change of G, the voltage is restricted within the upper boundary imposed by the algorithm. Thus the operating point is forced to stick near the MPP. As a result, there is a negligible deviation in the power. However it has to be acknowledged that the power is slightly lower than the actual PMPP. This is because the voltage stays close to the VMPP, not exactly on it. Nevertheless the difference is almost negligible and the efficiency is maintained well above 99%.

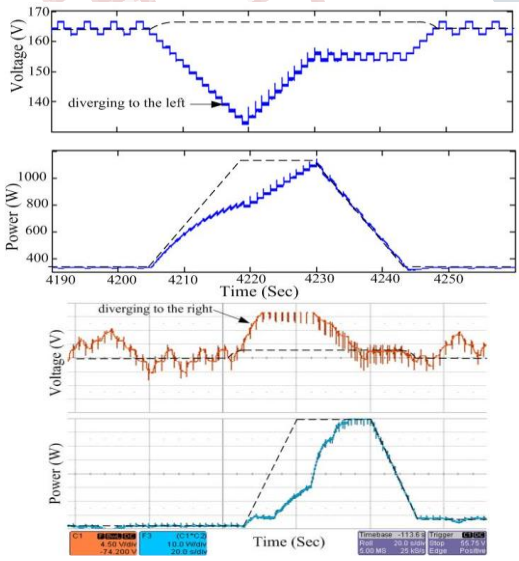

Fig. 9. The tracking performance of the conventional P&O for the 50 W/m2 ramp; (a) simulation (b) experimental

Fig. 10. The tracking performance of the modified P&O for the 50 W/m2 ramp; (a) simulation (b) experimental

In Fig. 9(a) and (b), the tracking performance of the conventional P&O for the 50 W/m^2 is presented. As expected, due to the faster ramp, the divergence worsens. The span of the deviation increases and the conventional P&O picks the MPP trail almost at the beginning edge of the descending *G* line. Due to this large deviation in the voltage, power also drops significantly. On the other hand, the modified P&O is consistent in following the power locus, as shown in Fig. 10. The results from simulation and experiment conclude that the imposed boundary successfully guides the operating point within the stipulated boundary that overcomes the power divergence issue.

VII. Conclusion

In this paper, a modified P&O algorithm is developed to increase the tracking efficiency. The approach is to simultaneously reduce the steady state oscillation while minimize the loss due to the losing direction. The key to the success of the algorithm is its ability to accurately detect the occurrence of oscillation and to introduce a boundary condition preventing it from being diverged away uncontrollably from the MPP. The performance of the proposed modified P&O is compared to the conventional one using the EN 50530 dynamic efficiency test. In all cases, the modified P&O performs better than the conventional by enhancing the efficiency by 1.1%

under the slow irradiance change and about 12% under the fast change. Since there modified version maintains the similar algorithm structure with the conventional, the former can be easily implementable with a low-cost 16/32 bit microcontroller. Thus it can be envisaged that this algorithm will draw considerable interest within the research and the industrial professionals in designing a new MPPT algorithm for the PV inverters.

VIII. REFERENCES

[1] T. Esram and P. L. Chapman, "Comparison of photovoltaic array maximum power point tracking techniques," *Energy Conversion, IEEE Transactions on*, vol. 22, pp. 439-449, 2007.

[2] Z. Salam, J. Ahmed, and B. S. Merugu, "The application of soft computing methods for MPPT of PV system: A technological and status review," *Applied Energy*, vol. 107, pp. 135-148, 2013.

[3] J. Ahmed and Z. Salam, "A critical evaluation on maximum power point tracking methods for partial shading in PV systems," *Renewable and Sustainable Energy Reviews*, vol. 47, pp. 933-953, 7, 2015.

[4] H. A. Sher, A. F. Murtaza, A. Noman, K. E. Addoweesh, K. Al-Haddad, and M. Chiaberge, "A New Sensorless Hybrid MPPTAlgorithm Based on Fractional Short-Circuit Current Measurement and P&O MPPT," *Sustainable Energy, IEEE Transactions on*, vol. PP, pp. 1-9, 2015.

[5] M. A. Elgendy, B. Zahawi, and D. J. Atkinson, "Assessment of Perturb and Observe MPPT Algorithm Implementation Techniques for PV Pumping Applications," *Sustainable Energy, IEEE Transactions on*, vol. 3, pp. 21-33, 2012.

[6] E. Koutroulis, K. Kalaitzakis, and N. C. Voulgaris, "Development of a microcontroller-based, photovoltaic maximum power point tracking control system," *Power Electronics, IEEE Transactions on*, vol. 16, pp. 46-54, 2001.

[7] M. Qiang, S. Mingwei, L. Liying, and J. M. Guerrero, "A Novel Improved Variable Step-Size Incremental-Resistance MPPT Method for PV Systems," *Industrial Electronics, IEEE Transactions on*, vol. 58, pp. 2427-2434, 2011.

[8] Syafaruddin, E. Karatepe, and T. Hiyama, "Artificial neural network-polar coordinated fuzzy controller based maximum power point tracking control under partially shaded conditions," *Renewable Power Generation, IET*, vol. 3, pp. 239-253, 2009.

[9] B. N. Alajmi, K. H. Ahmed, S. J. Finney, and B. W. Williams, "A Maximum Power Point Tracking Technique for Partially Shaded Photovoltaic Systems in Microgrids," *Industrial Electronics, IEEE Transactions on*, vol. 60, pp. 1596-1606, 2013.

[10] M. Seyedmahmoudian, R. Rahmani, S. Mekhilef, A. Maung Than Oo, A. Stojcevski, S. Tey Kok, *et al.*, "Simulation and Hardware Implementation of New Maximum Power Point Tracking Technique for Partially Shaded PV System Using Hybrid DEPSO Method," *Sustainable Energy, IEEE Transactions on*, vol. 6, pp. 850-862, 2015.

[11] K. Ishaque and Z. Salam, "A Deterministic Particle Swarm Optimization Maximum Power Point Tracker for Photovoltaic System Under Partial Shading Condition," *Industrial Electronics, IEEE Transactions on*, vol. 60, pp. 3195-3206, 2013.

[12] H. Renaudineau, F. Donatantonio, J. Fontchastagner, G. Petrone, G. Spagnuolo, J. P. Martin, *et al.*, "A PSO-Based Global MPPT Technique for Distributed PV Power Generation," *Industrial Electronics, IEEE Transactions on*, vol. 62, pp. 1047-1058, 2015.

[13] J. Ahmed and Z. Salam, "A Maximum Power Point Tracking (MPPT) for PV system using Cuckoo Search with partial shading capability," *Applied Energy*, vol. 119, pp. 118-130, 4/15/ 2014.

[14] F. Zhang, K. Thanapalan, A. Procter, S. Carr, and J. Maddy, "Adaptive hybrid maximum power point tracking method for a photovoltaic system," *Energy Conversion, IEEE Transactions on*, vol. 28, pp. 353-360, 2013.

[15] R. Alonso, P. Ibaez, V. Martinez, E. Roman, and A. Sanz, "An innovative perturb, observe and check algorithm for partially shaded PV systems," in *Power Electronics and Applications, 2009. EPE '09. 13th European Conference on*, 2009, pp. 1-8.

[16] S. K. Kollimalla and M. K. Mishra, "Variable Perturbation Size Adaptive P&O MPPT Algorithm for Sudden Changes in Irradiance," *Sustainable Energy, IEEE Transactions on*, vol. 5, pp. 718-728, 2014.

[17] A. Pandey, N. Dasgupta, and A. K. Mukerjee, "High-performance algorithms for drift avoidance and fast tracking in solar MPPT system," *Energy Conversion, IEEE Transactions on*, vol. 23, pp. 681-689, 2008.

[18] W. Xiao and W. G. Dunford, "A modified adaptive hill climbing MPPT method for photovoltaic power systems," in *Power Electronics Specialists Conference, 2004. PESC 04. 2004 IEEE 35th Annual*, 2004, pp. 1957-1963.

[19] F. Paz and M. Ordonez, "Zero oscillation and irradiance slope tracking for photovoltaic MPPT," *Industrial Electronics, IEEE Transactions on*, vol. 61, pp. 6138-6147, 2014.

[20] S. K. Kollimalla and M. K. Mishra, "Variable perturbation size adaptive P&O MPPT algorithm for sudden changes in irradiance," *Sustainable Energy, IEEE Transactions on*, vol. 5, pp. 718-728, 2014.

[21] M. Killi and S. Samanta, "Modified Perturb and Observe MPPT Algorithm for Drift Avoidance in Photovoltaic Systems," *Industrial Electronics, IEEE Transactions on*, vol. 62, pp. 5549-5559, 2015.

[22] R. Bründlinger, N. Henze, H. Häberlin, B. Burger, A. Bergmann, and F. Baumgartner, "prEN 50530–The New European Standard for Performance Characterisation of PV Inverters," in *Proc. 24th European Photovoltaic Solar Energy Conf*, 2009, pp. 3105-3109.

ISSN (Online) 2395-2717

International Journal of Engineering Research in Electrical and Electronic Engineering (IJEREEE)
Vol 3, Issue 12, December 2017

V.Poojitha has received her b.tech degree in electrical and electronics engineering from NBKR institute of science and technology (autonomous) vidyanagar, affiliated to JNTU A IN 2015.Pursuing m.tech degree in electrical power systems from audisankara college of engineering and technology (autonomous) gudur, affiliated to ananthapur JNTU in 2015-2017.

J.Suresh completed b.tech in electrical & electronic engineering from JNTU university, Hyderabad in 2001 affiliated to JNTU , Hyderabad and M.Tech in power system operation ans control from sree venkateswara university Tirupathi, in 2005. ph.D(EEE) from jawaharlal nehru technology university ananthapuram pre ph.D completed . working as a professor & HOD of the school of electrical and electronics engineering at audisankara college of engineering & technology, gudur